
Article:
de Carvalho, C.F. orcid.org/0000-0002-5780-5454, Planidin, N.P., Villoutreix, R. orcid.org/0000-0002-1815-3844 et al. (7 more authors) (2025) Ecology not genetic covariance explains correlated trait divergence during speciation. Molecular Ecology. e17818. ISSN 0962-1083

https://doi.org/10.1111/mec.17818

Supplemental Information for

Ecology not genetics explains correlated trait divergence during speciation

Authors: Clarissa F. de Carvalho[1,†*], Nicholas P. Planidin[2], Romain Villoutreix[2], Víctor Soria-Carrasco[3], Rüdiger Riesch[2,4], Jeffrey L. Feder[5], Tom Parchman[6], Jon Slate[1], Zachariah Gompert[7], Patrik Nosil[1,2,8*]

Affiliations:

[1]*School of Biosciences, University of Sheffield; Sheffield, S10 2TN, UK*

[2]*CEFE, Univ Montpellier, CNRS, EPHE, IRD; Montpellier, France*

[3]*John Innes Centre; Norwich, NR4 7UH, UK*

[4]*Department of Biological Sciences, Centre for Ecology, Evolution and Behaviour, Royal Holloway University of London; Egham, TW20 0EX, UK.*

[5]*Department of Biological Sciences, University of Notre Dame, Notre Dame, Indiana, 46556, USA*

[6]*Department of Biology, University of Nevada Reno; Reno, Nevada 89557, USA*

[7]*Department of Biology, Utah State University; Logan, Utah, 84322, USA*

[8]*SETE, Univ Université Paul Sabatier, CNRS, UMR-5321, F-09200 Moulis, France*

†*Present address: Departamento de Ecologia e Biologia Evolutiva, UNIFESP; Diadema, 09972-270, Brazil*

Email: clarissa.carvalho@unifesp.br; patrik.nosil@cefe.cnrs.fr

This PDF file includes:

Supporting text

Figures S1 to S6

Tables S1 to S8

Supporting text

Bayesian linear mixed models to test correlated trait divergence

While Mantel tests are appropriate for our distance-based analysis of non-autocorrelated color-pattern data (Guillot & Rousset, 2013; Legendre et al., 2015; Raufaste & Rousset, 2001), we implemented Bayesian linear mixed models (BLMMs) as a complementary approach to estimate the degree of association between color-pattern divergence and CHC divergence, which include random effects accounting for the pairwise nature of the variables (Clarke et al., 2002; Gompert et al., 2014). The Bayesian approach uses a Markov chain Monte Carlo framework to estimate the regression coefficients. The model was fitted via the *rjags* R package (Plummer, 2018), where divergence in color-pattern was the explanatory variable and each CHC trait was used as the response variable, separately. The variables were scaled and centered before the analyses. We ran three chains of the model, with 10,000 iterations, a burn-in of 2,000 iterations, and a thinning interval of 5.

Principal component analysis in the FHA population

To evaluate population structure in the FHA population, used for genetic covariance estimation, we conducted a principal component analysis (PCA). We included 183 striped and unstriped female individuals (excluding males and melanistic individuals) and performed PCA using the BIMBAM file in R (R Core Team, 2023). Results are shown in Fig. S1 and Fig. S2.

Jackknife re-sampling procedure

To evaluate the consistency of the genetic covariance estimates using genomic prediction across traits, we performed a jackknife re-sampling procedure. For each trait, we generated 100 jackknife replicates. In each replicate, we randomly sampled 95% of individuals from both the genotype and corresponding phenotype matrices, as well as 95% of SNPs, all without replacement. Individual identities were preserved and used to ensure matching between genotype and phenotype subsets.

Each replicate was analyzed using BSLMM implemented in *gemma* (Zhou et al., 2013). We ran five chains per replicate, each with 1,000,000 sampling steps, a burn-in of 200,000 steps; and minor allele frequency threshold of zero. The breeding values (BVs) were estimated on the model-averaged effect sizes, which incorporate both the main (sparse) effect and the polygenic component of SNP effects. We calculated the Pearson correlation of BVs across traits for each matching jackknife replicates, thereby generating a distribution of genetic covariances for each trait pair.

Bayesian hierarchical linear models to test phenotypic covariance

In addition to the phenotypic covariance tests between color-pattern and CHC traits, we performed Bayesian hierarchical linear models with the R package *brms* (Bürkner, 2017) by modeling the association between color-pattern morphs and the PCs describing CHC variation across the 10 populations. These models allowed us to pool data across populations while accounting for population-level random effects. Specifically, we fitted a Bayesian hierarchical linear model to assess the fixed effects of morph and sex on the principal component axes for each CHC trait. The model included random intercepts for population to account for population-level variability.

We used weakly informative priors for all parameters, with flat (uniform) priors for fixed effects (morph and sex) to allow the data to fully determine the posterior estimates. In addition, a Student's t (3, 0.3, 2.5) prior was assigned for the global intercept (hierarchical mean), and half-Student's t (3, 0, 2.5) priors were used for both the standard deviation of population-specific deviations (hierarchical standard deviation) and the residual standard deviation (sigma). The models were fitted using Hamiltonian Monte Carlo (HMC) sampling via the *brms* package in R, with 5 chains of 2000 iterations each (1000 warmup). All parameters showed good convergence, with Rhat values close to 1 and high effective sample sizes, suggesting reliable posterior sampling.

Genome-wide genetic differentiation between Timema *species*

To illustrate patterns of genetic differentiation representative of different species in *Timema*, we estimated patterns of genome-wide genetic differentiation between two *Timema* species that co-occur in nature: *T. californicum* and *T. poppensis* (Riesch et al., 2017). To this end, we used previously published whole genome sequence, using allele frequency estimates from sympatric populations of *T. californicum* and *T. poppensis* (locality LP, see Supplementary Table 3 from (Riesch et al., 2017) for 5,018,138 SNPs (filtered from a set of 5,074,942 SNPs to retain only SNPs with data for at least five individuals per species). The allele frequency estimates were taken directly from this past study and were based on an earlier, more fragmented genome assembly for a melanic *T. cristinae* with scaffolds combined into linkage groups based on inheritance patterns in mapping families (see Nosil et al., 2018).To quantify genetic differentiation, we estimated F_{ST} in 100 SNP windows as $F_{ST} = \Sigma_i(H_T-H_S)/\Sigma_i(H_T)$, where H_S and H_T are the mean subpopulation expected heterozygosity and the total expected heterozygosity given the mean allele frequencies, respectively. This analysis was conducted in R (R Core Team, 2023).

Patterns of CHC variation within and among Timema *species*

We conducted new analyses to summarize patterns of CHC variation within and among *Timema* species based on previously published data (Schwander et al., 2013). The data were obtained from Dryad (https://doi.org/10.5061/dryad.98f8c) and comprised relative abundances of seven cuticular hydrocarbons of the heptacosane class for 76 individuals from nine *Timema* species (stick insects were sampled from two populations in most species). Using R, we performed a PCA ordination of five of the CHCs (two of the CHCs were excluded as they were not scored in three species, *i.e.,* were missing data): 13Me27, 7Me27, 5Me27, 3Me27, 9Me27+11Me27 (these are all 27 carbon molecules with methyl (Me) groups on different carbons). For this analysis, we centered and standardized the CHC data. The first two PCs explained 54.2% and 21.9% of the CHC variation, respectively. 90% data ellipses for PC scores for each species were computed using the *ordiellipse* function in the R package *vegan* (Oksanen et al., 2022).

Supplementary Figures

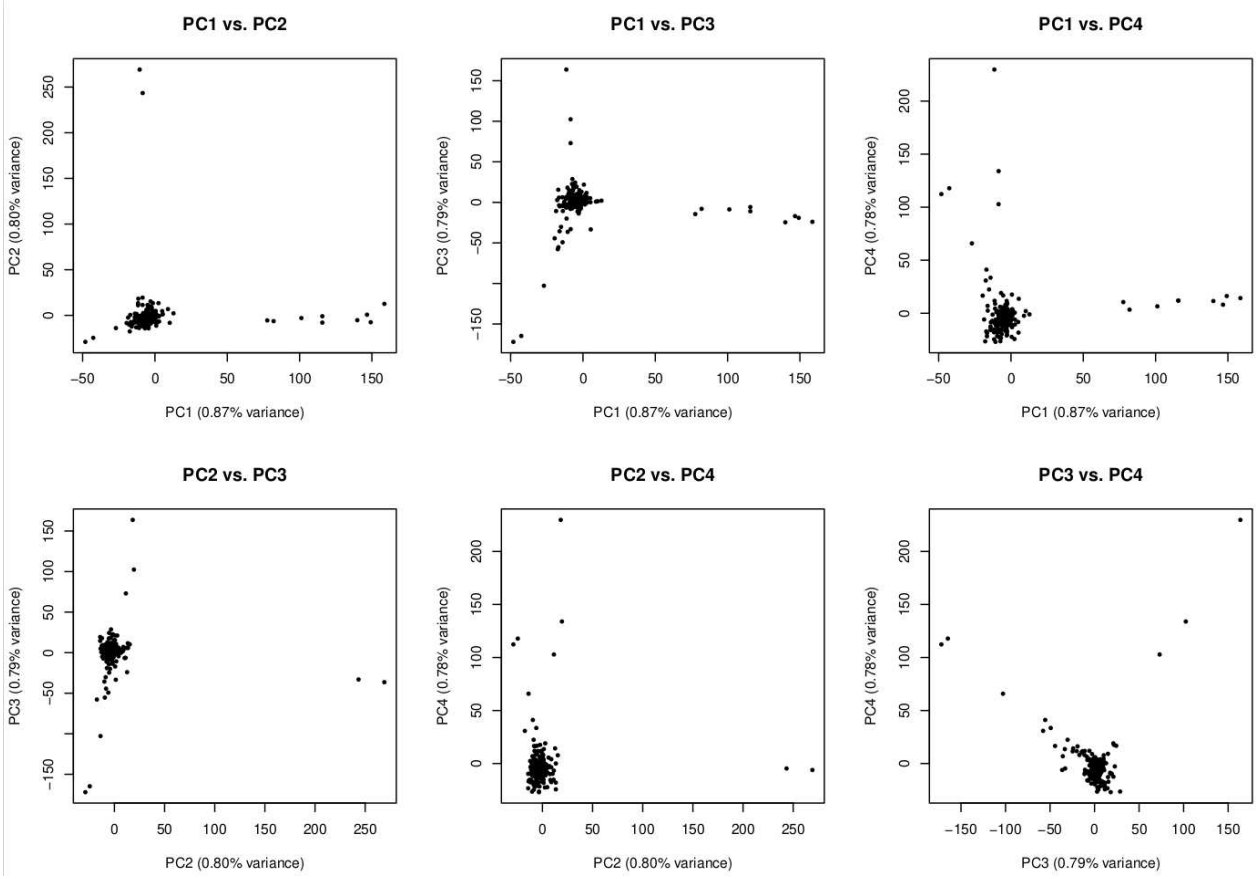

Figure S1. First four principal component axes for the 183 individuals used to estimate genetic covariance in FHA. The axes contribute minimally to the variance explained to the population, implying there is no population structure in FHA.

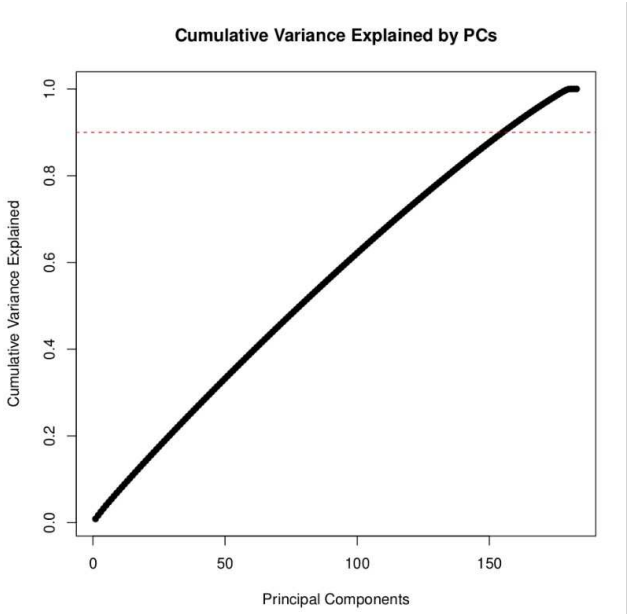

Figure S2. Cumulative variance explained by principal components (PCs) in FHA. The gradual increase in variance contribution with each PC suggests no significant population structure in FHA. Red line represents 90% of cumulative variance explained.

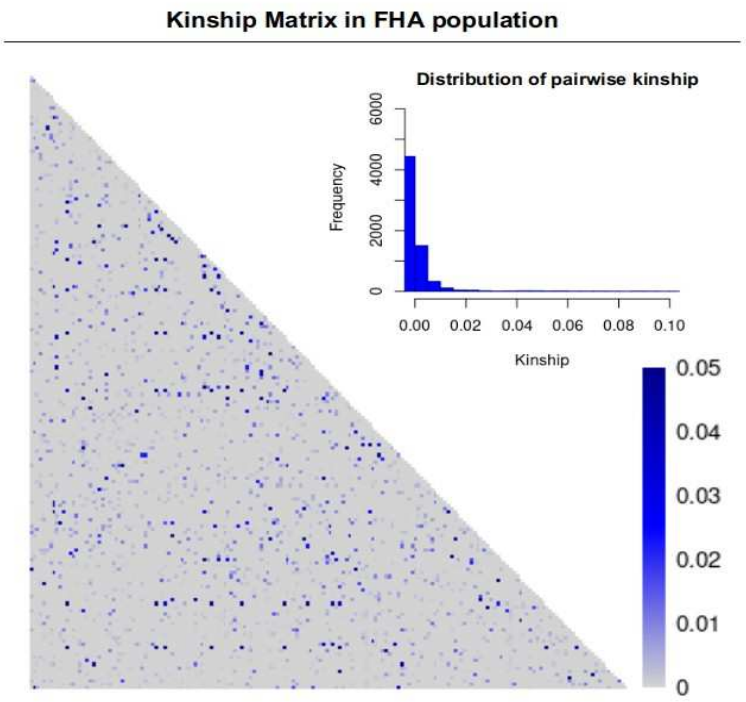

Figure S3. Kinship matrix for the 183 individuals used to estimate genetic covariance in FHA. The large panel displays the kinship matrix, showing generally low kinship values (near zero), as further highlighted in the smaller panel depicting the histogram of kinship values. The kinship matrix was estimated using *gemma,* which uses Bayesian sparse linear mixed models (BSLMM; Zhou et al., 2013).

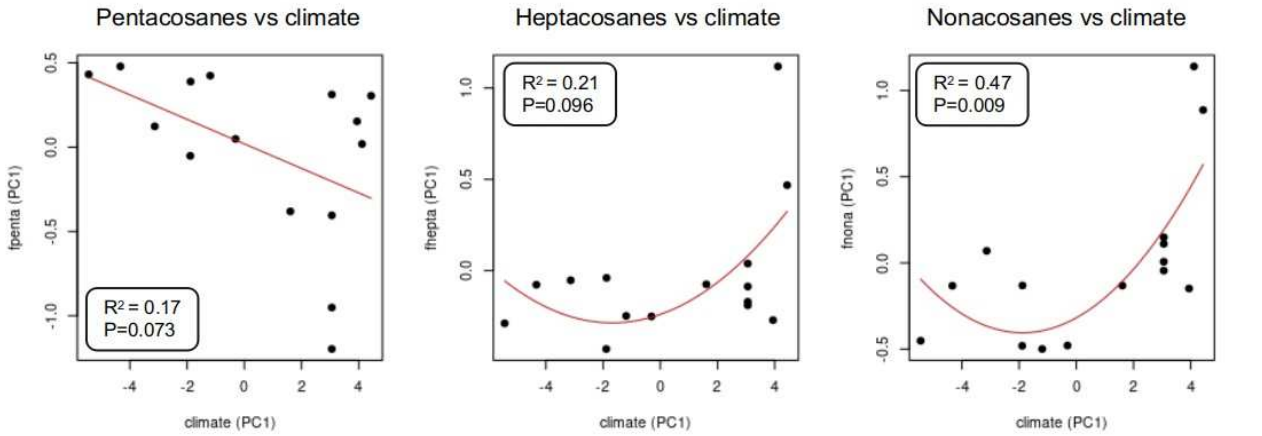

Figure S4. Association between female CHCs traits and climatic variables. CHCs traits from 15 populations (Table S2) were summarized for each CHC class using a principal component analysis (PCA). Here, we used the first PC axis (representing 50.3%, 88.5%, and 92.0% of the variation in female pentacosanes, heptacosanes, and nonacosanes, respectively). We used the first PC summarizing the 19 WorldClim bioclimatic variables to represent climatic variation (PC1 represents 67.9% of the variation). We used linear models to describe the regression, with the adjusted R^2 and corresponding p-value represented in each graph. Abbreviations: fpenta = female pentacosanes; fhepta = female heptacosanes; fnona = female nonacosanes.

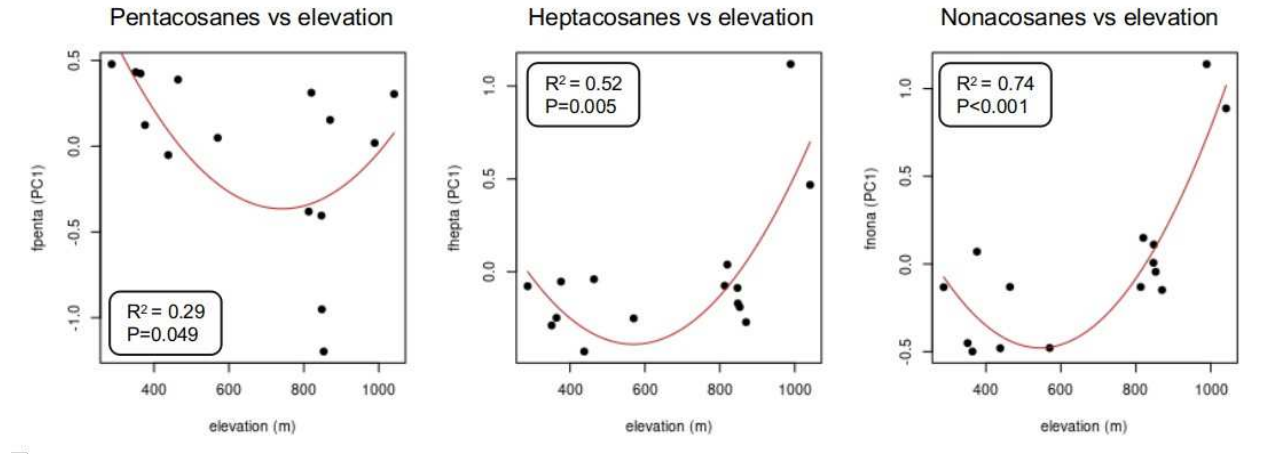

Figure S5. Association between female CHCs traits and elevation. CHCs traits from 15 populations (Table S2) were summarized for each CHC class using a principal component analysis (PCA), as in Fig. S1. We used linear models to describe the regression, with the adjusted R^2 and corresponding p-value represented in each graph. Abbreviations: fpenta = female pentacosanes; fhepta = female heptacosanes; fnona = female nonacosanes.

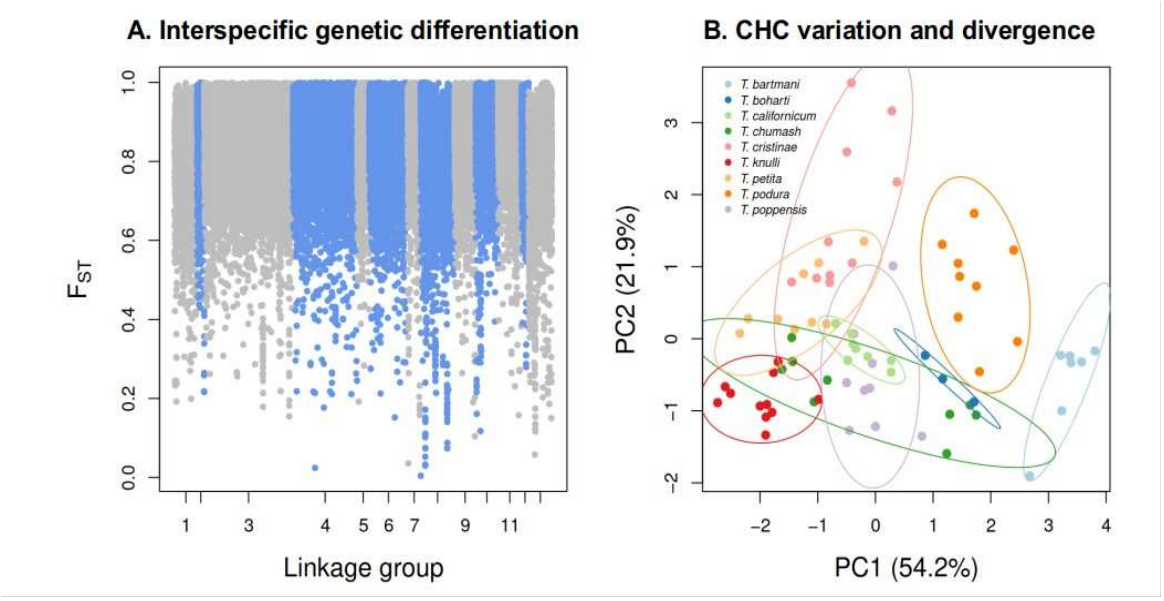

Figure S6. Species differences among *Timema*. (A) Manhattan plot depicting 100 SNP window estimates of F_{ST} between sympatric *Timema* species, *T. califonricum* and *T. poppensis*, from whole genome sequence data (data from Riesch et al., 2017). (B) Principal component analysis ordination of CHC variation within and among *Timema* species. Each point represents a stick insect and is colored by species. 90% data ellipses are shown for each species (data from Schwander et al., 2013).

Supplementary Tables

Table S1. The seven *T. cristinae* populations used to estimate divergence in color-pattern and in CHCs.

population code	locality	host	latitude	longitude	elevation (m)
LA	Laurel Springs	*Adenostoma*	34.509	-119.796	820
PRC	Paradise Road	*Ceanothus*	34.533	-119.857	364
MA	Mattress	*Adenostoma*	34.514	-119.800	848
PC	Poppy	*Ceanothus*	34.480	-119.770	287
OUTA	Outlook	*Adenostoma*	34.530	-119.840	464
OGC	Open Grass	*Ceanothus*	34.510	-119.800	847
HVA	Hidden Valley	*Adenostoma*	34.488	-119.787	376

Table S2. Phenotypic covariance between color-pattern and the principal components (PCs) summarizing variation in the different CHC compounds across populations. Column headers indicate the phenotypic covariance between color-pattern and the PCs for each CHC compound class (e.g., “PC1 penta” represents phenotypic covariance between color-pattern and PC1 for pentacosanes). P-values were estimated using permutation tests (n=1,000 permutations). No significant associations were observed (P> 0.05 for all tests).

Pop.	latitude	longitude	n	Prop. striped	PC1 penta	PC2 penta	PC1 hepta	PC1 nona	PC2 nona	PC3 nona
BYA	34.500	-119.860	19	0.79	0.09, P=0.08	0.06, P=0.52	0.02, P=0.43	-0.01, P=0.86	-0.02, P=0.61	-0.01, P=0.77
ECC20A	34.505	-119.733	19	0.74	-0.21, P=0.06	-0.09, P=0.29	-0.39, P=0.07	-0.32, P=0.08	-0.19, P=0.09	-0.14, P=0.13
ECC35A	34.506	-119.768	16	0.94	0.03, P=0.25	-0.01, P=0.87	0.00, P=1.00	-0.01, P=0.75	-0.01, P=0.62	-0.01, P=0.63
HVA	34.488	-119.787	11	0.73	-0.13, P=0.33	-0.14, P=0.31	0.00, P=0.95	0.05, P=0.49	0.05, P=0.31	0.04, P=0.37
MA	34.515	-119.797	14	0.79	-0.02, P=0.87	-0.01, P=0.86	0.00, P=0.92	-0.01, P=0.89	-0.02, P=0.73	-0.09, P=0.74
OGA	34.513	-119.796	14	0.79	0.14, P=0.53	0.11, P=0.49	-0.01, P=0.84	-0.03, P=0.46	-0.03, P=0.52	-0.08, P=0.64
OGC	34.513	-119.796	14	0.57	-0.06, P=0.68	-0.01, P=0.81	0.04, P=0.36	0.05, P=0.49	0.01, P=0.82	0.24, P=0.13
OUTA	34.532	-119.843	15	0.40	-0.10, P=0.10	-0.02, P=0.43	-0.05, P=0.16	0.00, P=0.98	-0.02, P=0.65	0.08, P=0.78
PC	34.477	-119.769	13	0.08	0.00, P=1.00	-0.06, P=1.00	0.00, P=0.84	0.01, P=1.00	0.15, P=0.70	0.09, P=0.46
R12C	34.515	-120.071	19	0.16	0.01, P=0.72	0.04, P=0.64	0.00, P=0.91	-0.04, P=0.18	-0.03, P=0.10	0.02, P=0.95

Abbreviations: Pop. = populations; n = number of samples (striped or unstriped), prop. striped = proportion of striped in dividuals among the samples, penta = pentacosanes, hepta = heptacosanes, nona = nonacosanes.

Table S3. Summary of the hyperparameters resulting from Bayesian sparse linear mixed models (BSLMM) to perform GWAS for color-pattern and CHC traits using *gemma*. The values represent the medians of the posteriors and the 95% ETPI values.

	h	**PVE**	**PGE**	**PVE x PGE**	**n-*y***
Stripe	0.94 [0.88, 0.97]	0.95 [0.92, 0.97]	0.99 [0.97, 1.00]	0.90 [0.85, 0.94]	46 [32, 61]
Pentacosanes	0.44 [0.04, 0.8]	0.39 [0.03, 0.76]	0.28 [0, 0.94]	0.16 [0.00, 0.57]	24 [0, 258]
Heptacosanes	0.29 [0.01, 0.74]	0.26 [0.01, 0.69]	0.29 [0, 0.95]	0.07 [0.00, 0.48]	44 [0, 276]
Nonacosanes	0.33 [0.02, 0.77]	0.29 [0.01, 0.7]	0.21 [0, 0.93]	0.08 [0.00, 0.49]	16 [0, 242]

h=estimated heritability; PVE=proportion of phenotypic variance explained by all single nucleotide polymorphisms (SNPs) in the model; PGE=proportion of PVE explained by SNPs with nonzero effects; gamma=number of SNPs with a measurable effect on the phenotype.

Table S4. *Timema cristinae* populations used to estimate the association between female CHCs and climate and elevation.

population	locality	host	latitude	longitude	elevation (m)
BYA	Brick yard	A	34.469	-119.677	870
ECC35A	East Camino Cielo 35	A	34.506	-119.768	1041
ECCCampA	East Camino Cielo Camp	A	34.506	-119.762	989
FHA	Far Hill	A	34.518	-119.801	813
HVA	Hidden Valley	A	34.488	-119.787	376
LA	Laurel Springs	A	34.509	-119.796	820
MA	Mattress	A	34.513	-119.796	848
OGA	Open Grass	A	34.513	-119.796	853
OGC	Open Grass	C	34.532	-119.843	847
OUTA	Outlook	A	34.477	-119.769	464
PC	Poppy	C	34.477	-119.769	287
PRC	Paradise Road	C	34.533	-119.857	364
R12C	Refugio 12	C	34.515	-120.071	351
R23A	Refugio 23	A	34.518	-120.077	438
SC	Stage Coach	C	34.523	-119.832	570

Abbreviations: A = *Adenostoma fasciculatum*; C = *Ceanothus spinosus*

Table S5. WorldClim bioclimatic variables, contribution to the different axes of the principal component analysis, and correlation with host plant. Correlations were estimated with Wilcoxon signed-rank test, and the table represents the corresponding *W-value* and *p-value*. The layer 14 (precipitation of the driest month) was excluded because it was zero across all localities. All correlations are significant, with the exception of between 'maximum temperature of warmest month' and host plant.

Worldclim bioclim layer	**PC**	**W**	**p-value**
Annual mean temperature	PC1	2686	1.39e-09
Mean diurnal range	PC2	3741.5	3.26e-04
Isothermality	PC1	3044.5	1.61e-07
Temperature seasonality	PC1	7431	2.38e-07
Max temperature of warmest month	PC2	4911	4.33e-01
Min temperature of coldest month	PC1	2800	7.58e-09
Temperature annual range	PC2	7008.5	2.82e-05
Mean temperature of wettest quarter	PC1	2682.5	1.43e-09
Mean temperature of driest quarter	PC2	3309	4.75e-06
Mean temperature of warmest quarter	PC2	3287.5	3.72e-06
Mean temperature of coldest quarter	PC1	2726	2.62e-09
Annual precipitation	PC1	7899	3.54e-10
Precipitation of wettest month	PC1	7274	1.34e-06
Precipitation seasonality	PC2	3090.5	2.12e-07
Precipitation of wettest quarter	PC1	7617.5	1.96e-08
Precipitation of driest quarter	PC1	7026	8.84e-07
Precipitation of warmest quarter	PC1	7757	1.84e-09
Precipitation of coldest quarter	PC1	7641.5	1.44e-08

Table S6. Summary of model comparison in Bayesian regressions evaluating the possible effects of different female CHC classes on sexual isolation (ipsi). Here, each class is evaluated alone. Among them, we evaluate pentacosanes (fpenta), heptacosanes (fpenta) and nonacosanes (fnona). We test the linear and quadratic models to explain sexual isolation. Values represented here are the deviance information criterion (DIC), and the best models are on top highlighted in bold.

model (fpenta vs ipsi)	**Deviance**	**pD**	**DIC**	**ΔDIC**
fpenta+fpenta²	38.73	6.59	**45.32**	0
fpenta	43.63	5.48	49.10	3.78
model (fnona vs ipsi)	**Deviance**	**pD**	**DIC**	**ΔDIC**
fhepta	60.83	3.95	**64.77**	0
fhepta+fhepta²	61.55	5.09	66.64	1.87
model (fnona vs ipsi)	**Deviance**	**pD**	**DIC**	**ΔDIC**
fnona	61.10	3.96	**65.06**	0.0
fnona+fnona²	61.05	5.05	66.10	1.04

Table S7. Summary of model comparison in Bayesian regressions evaluating the possible effects of different female CHC classes on sexual isolation, namely: pentacosanes (Fpenta), heptacosanes (Fpenta) and nonacosanes (Fnona), and geographical distance (Geo). Values represented here are the deviance information criterion (DIC), supporting Fpenta alone as the best model (β_{FPENTA}= 0.28 [-0.18, 0.72; 95% ETPI]). Here, we did not consider the quadratic relationship between the CHC classes and sexual isolation.

model	Deviance	pD	DIC	ΔDIC
Fpent	59.73	3.82	63.54	0.00
Geo	59.52	4.21	63.73	0.19
Geo+Fpent	58.99	4.94	63.93	0.39
Fnona	61.00	3.89	64.90	1.36
Geo+Fpent+Fnona	59.18	5.93	65.11	1.57
Fhept	61.12	4.00	65.12	1.58
Geo+Fnona	60.07	5.34	65.42	1.88
Fpent+Fnona	60.65	4.79	65.43	1.89
Fpent+Fhepta	60.76	4.85	65.62	2.08
Geo+Fhept	60.36	5.41	65.77	2.23
Geo+Fpent+Fhept	59.87	6.06	65.93	2.39
Fhept+Fnona	62.05	4.93	66.98	3.44
Geo+Fhept+Fnona	61.05	6.29	67.34	3.80
Fpent+Fhept+Fnona	61.67	5.95	67.62	4.08
Geo+Fpent+Fhept+Fnona	60.39	7.25	67.65	4.11

Table S8. Posterior estimates for Bayesian hierarchical linear model examining the effects of color-pattern morph and sex on the principal component axes of different CHC classes. Estimates are reported as posterior means with 95% credible intervals in brackets. Population was included as random effects, and in this table are reprsented as the standard deviation (SD) of the random effects. There is not a significant association between color-pattern morphs and any of the PCs describing CHC variation.

		PC1 penta	PC2 penta	PC1 hepta	PC1 nona	PC2 nona	PC3 nona
Fixed Effects	Intercept	-0.24 [-0.59, 0.09]	-0.44 [-0.86, -0.04]	0.09 [-0.21, 0.40]	0.48 [0.12, 0.87]	0.50 [0.04, 1.01]	0.47 [0.04, 0.93]
	Morph (striped)	-0.2 [-0.5, 0.11]	-0.06 [-0.36, 0.25]	-0.15 [-0.47, 0.16]	-0.15 [-0.49, 0.18]	-0.07 [-0.35, 0.19]	0.09 [-0.22, 0.40]
	Sex (male)	0.85 [0.6, 1.11]	0.94 [0.69, 1.19]	-0.07 [-0.34, 0.21]	-0.68 [-0.96, -0.42]	-0.86 [-1.07, -0.65]	-1.25 [-1.51, -0.99]
Random Effects	Population (SD)	0.32 [0.09, 0.65]	0.48 [0.25, 0.89]	0.20 [0.01, 0.48]	0.40 [0.17, 0.76]	0.68 [0.38, 1.19]	0.54 [0.28, 1.00]
Residual	sigma	0.83 [0.74, 0.93]	0.79 [0.70, 0.89]	0.90 [0.80, 1.01]	0.85 [0.76, 0.96]	0.67 [0.60, 0.75	0.82 [0.73,0.92]

Abbreviations: penta = pentacosanes, hepta = heptacosanes, nona = nonacosanes

Table S9. Population-specific random intercepts for the Bayesian hierarchical linear model examining the effects of color-pattern morph and sex on the principal component axes of different CHC classes. Estimates represent deviations from the overall intercept, with 95% credible intervals.

	Pop.	PC1 penta	PC2 penta	PC1 hepta	PC1 nona	PC2 nona	PC3 nona
Random effects per pop.	BYA	0.02 [-0.36, 0.38]	0.24 [-0.21, 0.70]	-0.08 [-0.42, 0.20]	-0.12 [-0.55, 0.29]	0.01 [-0.53, 0.52]	0.27 [-0.21 , 0.77]
	ECC20A	0.30 [-0.06, 0.73]	-0.65 [-1.14, -0.21]	0.22 [-0.06, 0.68]	0.46 [0.04, 0.93]	0.43 [-0.08, 0.95]	0.58 [0.09, 1.1]
	ECC35A	0.11 [-0.28, 0.5]	0.35 [-0.11, 0.85]	0.15 [-0.13, 0.57]	0.47 [0.01, 0.98]	0.44 [-0.07, 0.98]	0.50 [0.02, 1.05]
	HVA	-0.05 [-0.49, 0.36]	-0.22 [-0.73 , 0.26]	-0.04 [-0.39, 0.28]	-0.07 [-0.55, 0.40]	0.06 [-0.51, 0.62]	0.25 [-0.31, 0.81]
	MA	-0.32 [-0.79, 0.06]	-0.02 [-0.50, 0.45]	-0.01 [-0.35, 0.31]	0.02 [-0.44, 0.47]	0.19 [-0.35, 0.72]	0.07 [-0.43, 0.60]
	OGA	-0.37 [-0.85, 0.02]	-0.08 [-0.56, 0.41]	-0.01 [-0.33, 0.32]	-0.06 [-0.51, 0.37]	0.15 [-0.38, 0.72]	-0.63 [-1.18, -0.13]
	OGC	-0.14 [-0.56, 0.21]	-0.24 [-0.74, 0.22]	0.02 [-0.30, 0.37]	-0.03 [-0.48, 0.41]	0.12 [-0.44, 0.64]	-0.01 [-0.51, 0.50]
	OUTA	0.11 [-0.26, 0.52]	0.53 [0.06, 1.03]	-0.05 [-0.39, 0.25]	-0.21 [-0.67, 0.21]	0.10 [-0.44, 0.63]	-0.58 [-1.12 , -0.08]
	PC	0.24 [-0.17, 0.73]	-0.28 [-0.79, 0.21]	-0.03 [-0.39, 0.30]	-0.01 [-0.49, 0.45]	-1.53 [-2.13, -0.98]	-0.39 [-0.97, 0.14]
	R12C	0.07 [-0.32, 0.47]	0.37 [-0.09, 0.86]	-0.15 [-0.56, 0.12]	-0.50 [-1.00, -0.06]	-0.07 [-0.62, 0.45]	-0.08 [-0.60, 0.40]

Abbreviations: pop= population, penta = pentacosanes, hepta = heptacosanes, nona = nonacosanes

References

Bürkner, P.-C. (2017). brms: An R Package for Bayesian Multilevel Models Using Stan. *Journal of Statistical Software*, *80*, 1–28. https://doi.org/10.18637/jss.v080.i01

Clarke, R. T., Rothery, P., & Raybould, A. F. (2002). Confidence limits for regression relationships between distance matrices: Estimating gene flow with distance. *Journal of Agricultural, Biological, and Environmental Statistics*, *7*(3), 361–372. https://doi.org/10.1198/108571102320

Gompert, Z., Lucas, L. K., Buerkle, C. A., Forister, M. L., Fordyce, J. A., & Nice, C. C. (2014). Admixture and the organization of genetic diversity in a butterfly species complex revealed through common and rare genetic variants. *Molecular Ecology*, *23*(18), 4555–4573. https://doi.org/10.1111/mec.12811

Guillot, G., & Rousset, F. (2013). Dismantling the Mantel tests. *Methods in Ecology and Evolution*, *4*(4), 336–344. https://doi.org/10.1111/2041-210x.12018

Legendre, P., Fortin, M.-J., & Borcard, D. (2015). Should the Mantel test be used in spatial analysis? *Methods in Ecology and Evolution*, *6*(11), 1239–1247. https://doi.org/10.1111/2041-210X.12425

Nosil, P., Villoutreix, R., de Carvalho, C. F., Farkas, T. E., Soria-Carrasco, V., Feder, J. L., Crespi, B. J., & Gompert, Z. (2018). Natural selection and the predictability of evolution in Timema stick insects. *Science (New York, N.Y.)*, *359*(6377), Article 6377. https://doi.org/10.1126/science.aap9125

Oksanen, J., Simpson, G., Blanchet, F., Kindt, R., Legendre, P., Minchin, P., & et al. (2022). *The vegan package* [Computer software]. https://cran.r-project.org/package=vegan

Plummer, Martyn. (2018). rjags: Bayesian Graphical Models using MCMC. *R Package Version 4-8.* https://cran.r-project.org/package=rjags

R Core Team. (2023). *R: A language and environment for statistical computing.* [Computer software]. https://www.r-project.org/

Raufaste, N., & Rousset, F. (2001). Are Partial Mantel Tests Adequate? *Evolution*, *55*(8), 1703–1705. https://doi.org/10.1111/j.0014-3820.2001.tb00689.x

Riesch, R., Muschick, M., Lindtke, D., Villoutreix, R., Comeault, A. A., Farkas, T. E., Lucek, K., Hellen, E., Soria-Carrasco, V., Dennis, S. R., De Carvalho, C. F., Safran, R. J., Sandoval, C. P., Feder, J., Gries, R., Crespi, B. J., Gries, G., Gompert, Z., & Nosil, P. (2017). Transitions between phases of genomic differentiation during stick-insect speciation. *Nature Ecology and Evolution*, *1*(4), Article 4. https://doi.org/10.1038/s41559-017-0082

Schwander, T., Arbuthnott, D., Gries, R., Gries, G., Nosil, P., & Crespi, B. J. (2013). Hydrocarbon divergence and reproductive isolation in Timema stick Insects. *BMC Evolutionary Biology*, *13*(1). https://doi.org/10.1186/1471-2148-13-151

Zhou, X., Carbonetto, P., & Stephens, M. (2013). Polygenic Modeling with Bayesian Sparse Linear Mixed Models. *PLoS Genetics*, *9*(2), e1003264. https://doi.org/10.1371/journal.pgen.1003264